

Nonlinear Vibrations of Chains

FRIEDRICH PFEIFFER

PETER FRITZ

JÜRGEN SRNIK

Lehrstuhl B für Mechanik, Technische Universität München, Luisenstr. 37a, 80290 München, Germany

(Received 21 June 1996, accepted 16 October 1996)

Abstract: Chains are important machine components in cars, in gears, and in armored vehicles. The dynamics of chains typically are characterized by free motion and contact processes, which may include impacts and friction. Therefore, modeling by multibody theory augmented by methods of contact mechanics represents an appropriate way to evaluate dynamic chain behavior. This paper gives some examples.

Key Words: Continuous variable transmission, roller chain drive, multibody dynamics, complementary contact problem

1. INTRODUCTION

Typically, chains consist of chain elements that might be connected by ideal joints, joints with backlash, or journal bearing joints. Furthermore, and considering continuous variable transmission systems (CVT), chains may be connected by rocker pins or more complicated pin systems. Chains come into contact with guides and sprocket wheels, or they make contact with controllable sheaves. In the case of vehicles, chains make sprocket and ground contact. In all cases, contacts start by nullifying the relative distance between a guide, sprocket, or sheave and some chain element, and end by nullifying some force condition like normal force or static friction force. In between, contacts possess sliding friction or stick-slip transition, and local separation and closure might occur again. Altogether, all types of mechanical contact phenomena may occur between chains and their controlling elements.

Traditionally, chains have been modeled as a kind of uniform string (Fritzer, 1992; Yue, 1992) because the methods available could hardly deal with chains composed of single elements. Nevertheless, polygonal effects were considered in Mahaligham (1958) and Chen and Freudenstein (1988). The basic work of Binder (1956) described the various possibilities of eigenfrequencies and parametric excitations. None of these contributions regarded contact processes between chains and their controlling elements such as sprockets, guides, or sheaves. In an approximative way, Naja and Marshek (1983) analyzed the contact forces for a steady-state behavior depending on the stress ratio between the tight and slack span. Nakanishi and Shabana (1994) developed very detailed chain models including contact forces for links, sprockets, and idlers with special application to large-scale tracked vehicles.

At the Technische Universität München, a series of studies were performed that dealt with contact problems in multibody systems (Pfeiffer, 1984; Prestl, 1991; Seyfferth and Pfeiffer, 1992; Glocker and Pfeiffer, 1993, 1995; Pfeiffer and Glocker, 1996). These findings form a sound basis for analyzing chains (Fritz and Pfeiffer, 1995; Srnik and Pfeiffer, 1994).

2. CONTACT DYNAMICS

Multibody systems such as chains with multiple unilateral contacts may be influenced dynamically by stick-slip phenomena and impulsive processes. Such events are indicated by kinematical magnitudes such as relative distances or relative velocities, which become constraints when the contact event occurs. Examples include a closing contact or a transition from sliding to stiction. Constraints generate constraint forces that, for an existing (active) contact situation such as contact of two bodies or stiction, serve as an indicator for the duration of the event. For example, a contact separates when the normal constraint force changes sign or when stiction breaks down for static friction forces smaller than the tangential constraint forces. Designating $\mathbf{g}_N \in \mathbb{R}^{n_N}$ as the vector of relative distances in n_N contacts and $\dot{\mathbf{g}}_H \in \mathbb{R}^{n_H}$ as the vector of relative velocities in n_H contacts, we may write the appropriate equations of motion in the following form (Glocker and Pfeiffer, 1995):

$$\begin{aligned} M\ddot{\mathbf{q}} - \mathbf{h} - \left(\mathbf{W}_N + \mathbf{W}_G \mu_G : \mathbf{W}_H \right) (\lambda_N \lambda_H) &= \mathbf{0} \in \mathbb{R}^f \\ (\ddot{\mathbf{g}}_N \ddot{\mathbf{g}}_H) &= (\mathbf{W}_N^T \mathbf{W}_H^T) \ddot{\mathbf{q}} + (\bar{\mathbf{w}}_N \bar{\mathbf{w}}_H) \in \mathbb{R}^{n_N+n_H}, \end{aligned} \tag{1}$$

where $M \in \mathbb{R}^{f,f}$ is the mass matrix, $\mathbf{q} \in \mathbb{R}^f$ are the generalized coordinates, $\mathbf{h} \in \mathbb{R}^f$ are all forces except constraint forces, $\mathbf{W}_N \in \mathbb{R}^{f,n_N}$, $\mathbf{W}_H \in \mathbb{R}^{f,n_H}$, $\mathbf{W}_G \in \mathbb{R}^{f,n_N-n_H}$ are constraint matrices, $\bar{\mathbf{w}}_N \in \mathbb{R}^{n_N}$, $\bar{\mathbf{w}}_H \in \mathbb{R}^{n_H}$ are constraint vectors (mostly excitation terms), $\mu_G = \text{diag}\{-\mu_i \text{sgn } \dot{g}_{Ti}\}$ is the sliding friction coefficient matrix, and $\lambda_N \in \mathbb{R}^{n_N}$, $\lambda_H \in \mathbb{R}^{n_H}$ are constraint forces (Lagrange vectors). The constraint equations for \mathbf{g}_N and $\dot{\mathbf{g}}_H$ were placed in second-order form. The different sets can conveniently be characterized in the following form:

$$\begin{aligned} I_G &= \{1, 2, \dots, n_G\} \\ I_S &= \{i \in I_G \mid g_{Ni} = 0\} \text{ with } n_S \text{ elements} \\ I_N &= \{i \in I_S \mid \dot{g}_{Ni} = 0\} \text{ with } n_N \text{ elements} \\ I_H &= \{i \in I_H \mid \dot{g}_{Ti} = 0\} \text{ with } n_H \text{ elements.} \end{aligned} \tag{2}$$

In our multibody system, there are n_G contacts. In n_S contacts, the relative distance $g_{Ni} = 0$, but in n_N contacts the relative velocity \dot{g}_{Ni} is also zero. Stick-slip might happen only for such contacts, whereas stiction takes place in n_H contacts. Consequently, sliding friction develops only in $(n_N - n_H)$ contacts for $i \in I_N \setminus I_H$. Combining further,

$$\begin{aligned} \ddot{\mathbf{g}} &= (\ddot{\mathbf{g}}_N \ddot{\mathbf{g}}_H) \quad \lambda = (\lambda_N \lambda_H) \quad \bar{\mathbf{w}} = (\bar{\mathbf{w}}_N \bar{\mathbf{w}}_H) \\ \mathbf{W} &= \left(\mathbf{W}_N : \mathbf{W}_H \right) \quad \mathbf{N}_G = \left(\mathbf{W}_G \mu_G : \mathbf{0} \right), \end{aligned} \tag{3}$$

we write equation (1):

$$\begin{aligned} \mathbf{M}\ddot{\mathbf{q}} - \mathbf{h} - (\mathbf{W} + \mathbf{N}_G)\lambda &= \mathbf{0} \in \mathbb{R}^f \\ \ddot{\mathbf{g}} &= \mathbf{W}^T\ddot{\mathbf{q}} + \ddot{\mathbf{w}} \in \mathbb{R}^{n_N+n_H} \end{aligned} \tag{4}$$

which can be solved for $(\ddot{\mathbf{q}}, \lambda)$ for time instants in which no transitions or separations occur. In this special case, $\ddot{\mathbf{g}} = \mathbf{0}$, and we end up with

$$[\mathbf{W}^T\mathbf{M}^{-1}(\mathbf{W} + \mathbf{N}_G)]\lambda = -(\mathbf{W}^T\mathbf{M}^{-1}\mathbf{h} + \ddot{\mathbf{w}}), \tag{5}$$

which results in the unknown vector λ . From the first equation (4), we can then evaluate $\ddot{\mathbf{q}}$.

In cases of transitions or separations, the sets (1) or (4) cannot be evaluated in a straightforward way. In multiple contact situations, every change of only one contact might influence all other contacts. It is not known beforehand what combination of constraints in all other contacts will follow such a change. We could start a combinatorial search to solve this problem. A more elegant way consists of a complementarity formulation (Lemke, 1970; Pfeiffer, 1993) by applying a basic law of contact mechanics. This law states, roughly, that in mechanical contacts, either magnitudes of relative kinematics are zero and the thus generated constraint forces are not zero or vice versa. The product of these two groups of magnitudes is always zero.

To apply this law to our chain problem, we start with equation (1), in which the kinematical constraints are expressed on an acceleration level. The above law means that for normal contacts,

$$\ddot{\mathbf{g}}_N \geq \mathbf{0} \quad \lambda_N \geq \mathbf{0} \quad \ddot{\mathbf{g}}_N^T \lambda_N = 0. \tag{6}$$

These are n_N inequalities for $(\ddot{\mathbf{g}}_N, \lambda_N)$ and one complementarity condition. For stick-slip processes, a complementarity form is much more complicated to establish because we must consider very thoroughly the properties of the friction cone in each contact. For a contact i , we have with $\ddot{\mathbf{g}}_H = \{\ddot{g}_{Ti}\}$ and $\lambda_H = \{\lambda_{Ti}\}$:

$$\lambda_{Ni} \geq 0; \left. \begin{aligned} |\lambda_{Ti}| < \mu_{0i}\lambda_{Ni} &\Rightarrow \ddot{g}_{Ti} = 0 \\ \lambda_{Ti} = +\mu_{0i}\lambda_{Ni} &\Rightarrow \ddot{g}_{Ti} \leq 0 \\ \lambda_{Ti} = -\mu_{0i}\lambda_{Ni} &\Rightarrow \ddot{g}_{Ti} \geq 0 \end{aligned} \right\} i \in I_H. \tag{7}$$

The inequalities (7) can be put in a standard complementarity form by a rather tedious decomposition procedure (Glocker and Pfeiffer, 1993). We can always combine equations (1), (6), and (7) in a final set to form a linear complementarity problem in its standard form (Lemke, 1970):

$$\mathbf{y} = \mathbf{A}\mathbf{x} + \mathbf{b} \quad \mathbf{y} \geq \mathbf{0} \quad \mathbf{x} \geq \mathbf{0} \quad \mathbf{y}^T \mathbf{x} = \mathbf{0} \quad \mathbf{y}, \mathbf{x} \in \mathbb{R}^{n_N+4n_H}. \tag{8}$$

Note that for general spatial contact problems, a formulation of a linear complementarity problem cannot be achieved. Spatial contact problems are connected with two tangential force directions in the plane of contact. As a consequence, the direction of motion after a

transition stick to slip, for example, depends on the geometric sum of two tangential forces, which thus generate a nonlinear complementarity form (Pfeiffer and Glocker, 1996).

To describe our chain problem, we need an impact analysis in its simplest form; namely, frictionless impacts by Newton’s law. Starting again with equation (1) and setting $\ddot{\mathbf{g}}_H, \lambda_H = 0$, we end up with

$$\mathbf{M}\ddot{\mathbf{q}} - \mathbf{h} - \mathbf{W}_N \lambda_N = 0 \quad \ddot{\mathbf{g}}_N = \mathbf{W}_N^T \ddot{\mathbf{q}} + \ddot{\mathbf{w}}_N. \tag{9}$$

Integrating these equations in the interval (t_A, t_E) with $t_E \rightarrow t_A$, defining $\dot{\mathbf{g}}_{NA} = \dot{\mathbf{g}}_N(t_A)$, $\dot{\mathbf{q}}_A(t_A)$ and so forth, and applying Newton’s impact law,

$$\dot{\mathbf{g}}_{NE} = -\varepsilon_N \dot{\mathbf{g}}_{NA} \text{ with } \varepsilon_N = \text{diag}(\varepsilon_{N_i}), \tag{10}$$

we finally get the result

$$\begin{aligned} M(\dot{\mathbf{q}}_E - \dot{\mathbf{q}}_A) - \mathbf{W}_N \Lambda_N &= 0 \\ \dot{\mathbf{g}}_{NA} = \mathbf{W}_N^T \dot{\mathbf{q}}_A + \tilde{\mathbf{w}}_N, \dot{\mathbf{g}}_{NE} &= \mathbf{W}_N^T \dot{\mathbf{q}}_E + \tilde{\mathbf{w}}_N \\ \Lambda_N &= \lim_{t_E \rightarrow t_A} \int_{t_A}^{t_E} \lambda_N dt. \end{aligned} \tag{11}$$

Combining equations (10) and (11), we calculate the generalized velocity $\dot{\mathbf{q}}_E$ after an impact and the impulse Λ_N :

$$\begin{aligned} \dot{\mathbf{q}}_E &= \dot{\mathbf{q}}_A - \mathbf{M}^{-1} \mathbf{W}_N \mathbf{G}_N^{-1} (\mathbf{E} + \varepsilon_N) \dot{\mathbf{g}}_{NA} \\ \Lambda_N &= -\mathbf{G}_N^{-1} (\mathbf{E} - \varepsilon_N) \dot{\mathbf{g}}_{NA} \\ \text{with } \mathbf{G}_N &= \mathbf{W}_N^T \mathbf{M}^{-1} \mathbf{W}_N. \end{aligned} \tag{12}$$

The initial relative velocity \mathbf{g}_{NA} is given with equation (11). With these equations, all the tools necessary for analyzing chains are available. We shall therefore concentrate in the following on the determination of the special matrices and vectors.

3. CHAIN AND CHAIN ELEMENTS

3.1. General Remarks

In modeling chains and chain elements, we first must choose convenient coordinate frames. We start with an inertial coordinate base chosen in such a way that the geometry to the elements becomes as simple as possible; for example, located in the centers of sprockets or sheaves. We further fix at each element (chain element, sheave, sprocket, guides) a moving body fixed coordinate system at a convenient point, for example, in the mass center. Sometimes it might be convenient to have a second body-related frame that is inertially fixed with one axis and rotates with a nominal speed, for example, for shafts and wheels. The system of coordinate frames must allow a complete and unambiguous geometrical description of all system elements.

Second, we must define a nominal motion that is nontrivial for chain dynamics. We start with a prescribed (time dependent or not) motion of the driving component, for example, one

sprocket or one pulley. But we have to decide what a nominal motion of the chain system might look like. One could go back to the stringlike model as developed earlier, which is a reasonable basis. A more advanced nominal motion can be evaluated by taking into account the discrete chain structure and thus the polygonal effects and by not considering the detailed friction and impact phenomena. Experience shows that this approach seems to give good results and, moreover, a sound basis for more refined investigations.

3.2. Links and Joints

Typical links and joints for chains are very similar in different applications, such as roller chains in cars, rocker pin chains in CVT gears, or even chains in tracked vehicles. The chain elements consist of a link that is connected to the neighboring link by a pin, a bushing, a rocker pin, or some similar object. In all cases, these connections possess backlash that leads to relative motion. In roller chains or in CVT chains, the chain pins are lubricated by oil. They behave like a journal bearing and can be modeled as such. In many cases, it might even be sufficient to assume ideal joints being conveniently described by kinematical constraint equations. For heavy-tracked vehicles, the connections of the chain elements are not lubricated, and the rather large backlashes generate impulsive noise. We shall not consider this case here.

A typical chain element is shown in Figure 1. In general, every element possesses six degrees of freedom, although in most applications it will be sufficient to consider only three degrees of freedom (two degrees-of-freedom translations, one degree-of-freedom rotation).

From Figure 1, we get the coordinates of the link

$${}^L\mathbf{r} = \begin{pmatrix} {}^Lx \\ {}^Ly \\ {}^Lz \end{pmatrix} \quad {}^L\varphi = \begin{pmatrix} {}^L\alpha \\ {}^L\beta \\ {}^L\gamma \end{pmatrix} \quad {}^L\mathbf{q} = \begin{pmatrix} {}^L\mathbf{r} \\ {}^L\varphi \end{pmatrix}, \quad (13)$$

which of course might be written down in any coordinate frame. For the following roller chain and CVT models, we consider only the plane case (${}^Lz = 0, {}^L\alpha = 0, {}^L\beta = 0$).

For the chain joints, we may either use an ideal joint model, which reduces further the number of degrees of freedom to one (namely, ${}^L\varphi$), and two additional geometrical constraints for \mathbf{r}_L . This leads to

$${}^L\varphi = \begin{pmatrix} 0 \\ 0 \\ {}^L\gamma \end{pmatrix} \quad {}^L\mathbf{r} = {}^L\mathbf{r}({}^L\mathbf{q}) = \begin{pmatrix} {}^Lx \\ {}^Ly \\ 0 \end{pmatrix}. \quad (14)$$

Alternatively, we may apply an approximation as a journal bearing with symmetric stiffness and damping matrices (Figure 2).

3.3. Contact and Controlling Elements

CVT chains are controlled by movable and nonmovable sheaves; roller chains are controlled by sprockets and guides. The contact processes in the first case include impacts at the sheave

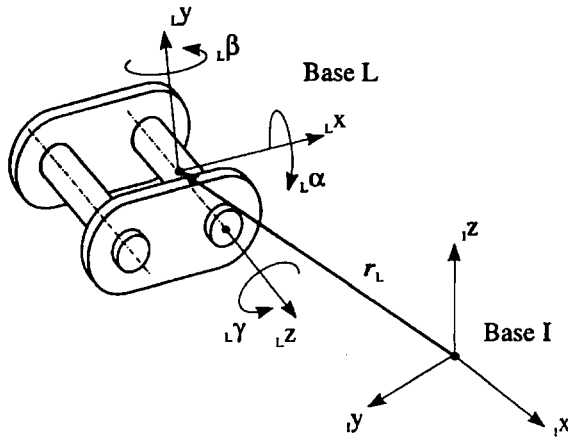


Figure 1. Typical chain link.

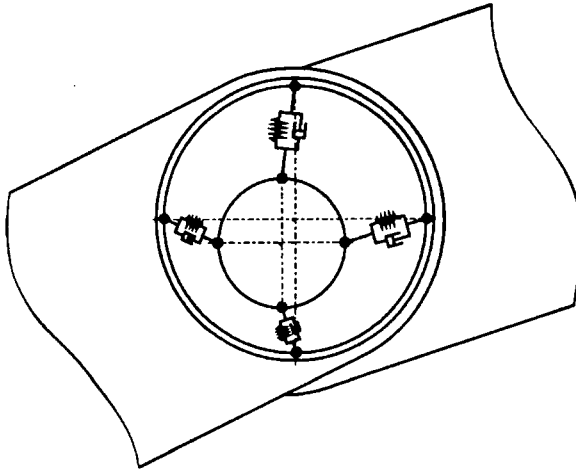


Figure 2. Chain connection as a journal bearing.

entry and stick-slip phenomena during sheave contact. At the pulley exit, we might observe impulsive effects when the chain rocker pins leave the pulley. In the second case of roller chains, we observe not stick-slip processes but more sliding friction effects. Instead, we observe more impulsive processes on the guides and when entering or leaving the sprockets. Separation effects with subsequent contacts might occur along the guides. All effects are covered by the above theory. Nevertheless, we shall look into some details.

Figure 3 illustrates a typical configuration of a CVT gear. The chain elements may have contact with one pulley and are moving without such contacts in the strands between the two pulleys. Pulley 1 is the driving wheel. During motion, the rocker pin contacts with the pulley cones change. The rocker pin itself is modeled as one bolt with linear axial stiffness. We assume that Coulomb's law can be applied in the contact zone, and we know that the rocker pin moves within the conical pulley in two directions: radial

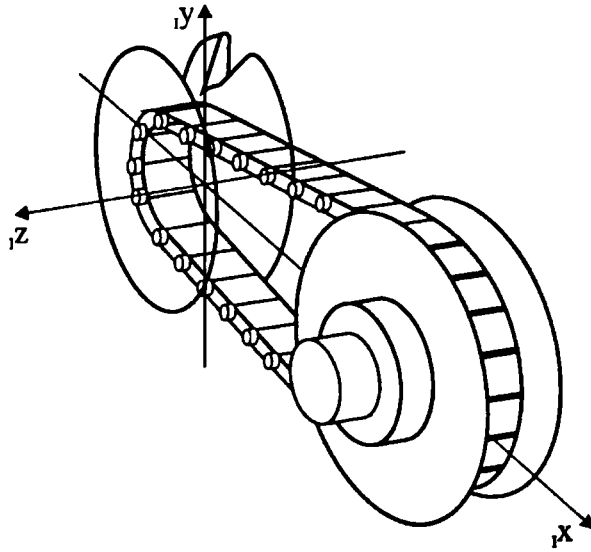


Figure 3. Typical CVT configuration.

and circumferential. This gives rise to a two-dimensional contact problem with nonlinear complementarity properties (Figure 4). With respect to Coulomb’s law, in this case, it turned out that computing time could be reduced significantly by approximating the dry friction characteristic by a continuous function.

The relative normal distance $g_{Ni}(\mathbf{q}, t)$ and the relative tangential velocity $\dot{g}_{Ti}(\mathbf{q}, \dot{\mathbf{q}}, t)$ must be expressed in generalized coordinates and included in equation (1). The forces F_r, F_t in radial and circumferential directions depend on the constraint force vectors (λ_N, λ_H) . Note that $g_{Ni}(\mathbf{q}, t)$ results from the approaching motion of the rocker pin as part of a strand element when coming nearer to the pulley.

The mechanical models for the pulleys are comparatively simple and very similar to those of sprockets. In both cases, we have wheels with three degrees of freedom in a plane model and six degrees of freedom in a spatial model. Stiffness and damping of the wheel bearings depend on their design, for example, roller or journal bearings (Figure 5):

$${}_w\mathbf{r} = \begin{pmatrix} {}_wx \\ {}_wy \\ {}_wz \end{pmatrix} \quad {}_w\varphi = \begin{pmatrix} {}_w\alpha \\ {}_w\beta \\ {}_w\gamma \end{pmatrix} \quad {}_w\mathbf{q} = \begin{pmatrix} {}_w\mathbf{r} \\ {}_w\varphi \end{pmatrix}, \tag{15}$$

where the index W stands for sprocket or sheave and the angles ${}_w\varphi$ of deviation are small. In the plane case, ${}_wz = 0, {}_w\alpha = 0, {}_w\beta = 0$.

The forces acting on a sheave are either external torques on the pulley shaft or internal forces coming from the contacts with the rocker pins. The latter is defined in Figure 4. Regarding a sprocket, again we have to consider the external torques from the camshafts and the rotational vibrations of the crankshaft. Besides the chain forces between the links, additional contact forces act on the chain bolts and on the sprocket tothing (Figure 6).

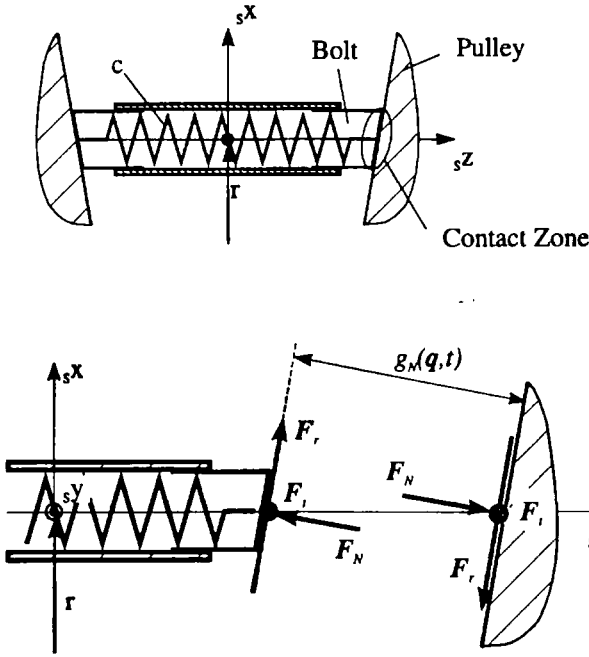


Figure 4. Rocker pin contacts.

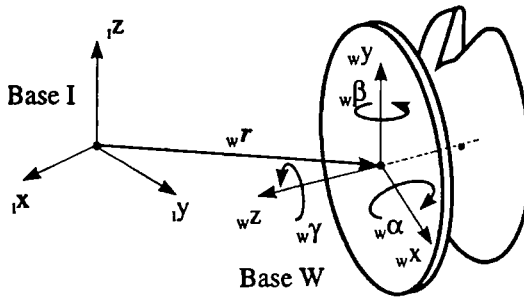


Figure 5. Wheel kinematics.

Particularly, the impulsive forces due to the polygonal excitation, when a link enters the sprocket, influence the sprocket dynamics and the dynamics of the chain strands.

Guides (Figure 7) are used in chain drives to reduce the vibrations of the chain strands and to preload the chain with a definite stress, which is produced by some tension device. Therefore, guides develop their own dynamics so that the links might lose their contact with the guide. At each contact of the links, forces in normal and tangential directions act on the guide and the link plate. Again, we have to calculate the impulsive forces when a contact between a link and a guide becomes active.

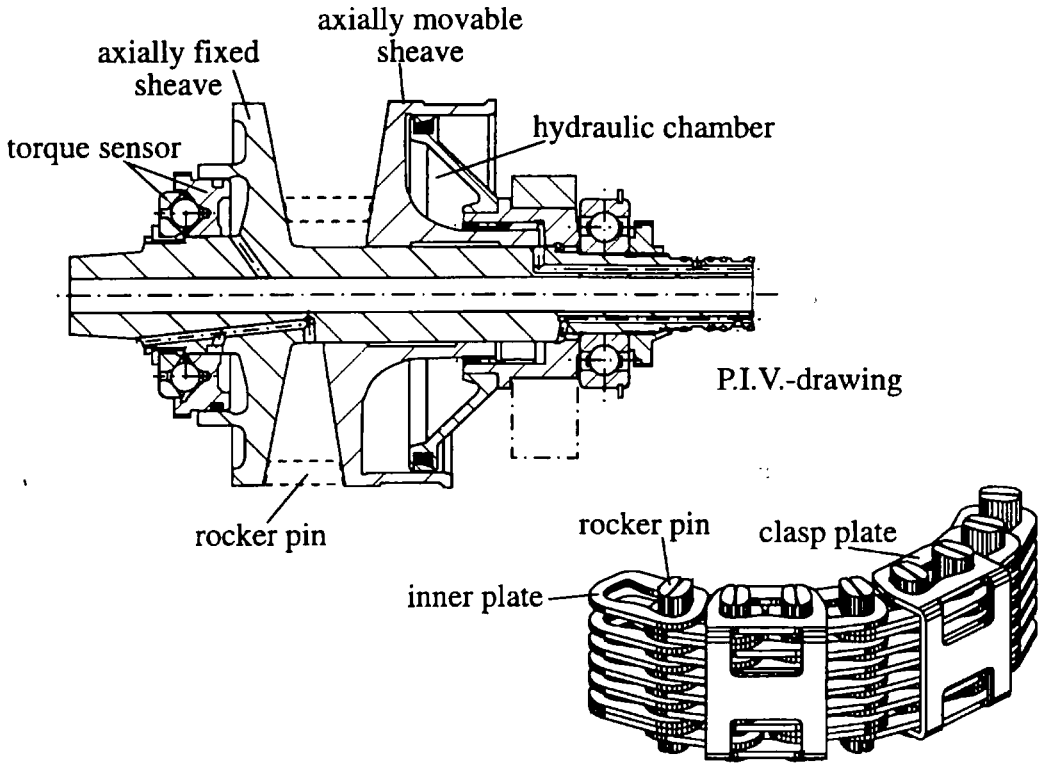


Figure 8. CVT chain drive components.

The mechanical model takes into account the plain motion of the 63 links with 189 degrees of freedom, the driven pulley with 1 rotational degree of freedom and a torsional excitation, and the driving pulley with 0 degrees of freedom and a torsional excitation. An arbitrary ratio of transmission can be applied.

The results were computed for a stationary working order with constant driving speed and output torque on geared level. Computing time for this case amounts about 8 hours on a SUN workstation. Figure 9 shows the contact forces acting on a pair of rocker pins during one revolution and the tensile force in the related chain link.

As long as the chain link is part of a strand, no contact forces work on its rocker pins. When it comes into contact with one of the pulleys, the pins are pressed between the two sheaves, and hence the normal force increases. Its amplitude depends on the geometry of the sheaves and the transmitted power. The frictional force is a function of this normal force and the relative velocity between the pulley and the pins. It is split into one radial and one circumferential component. The radial contact force coincides with a radial movement of the chain link that equals a power dissipation. In contrast, the circumferential contact force causes the changes of the tensile force in the corresponding chain link, which leads to different tensile force levels in the two strands that agree with the transmitted torque.

Due to the mechanical model, the simulation provides an integrated value of the tensile force in the plates of a chain link, whereas measurement was performed for the tensile

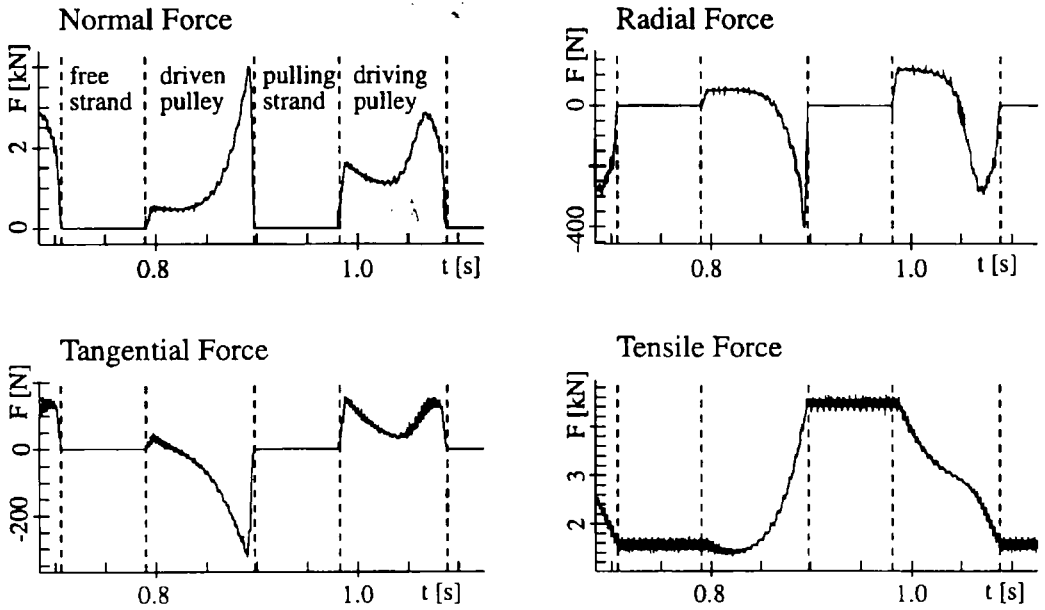


Figure 9. Forces acting on the rocker pins and in a chain link.

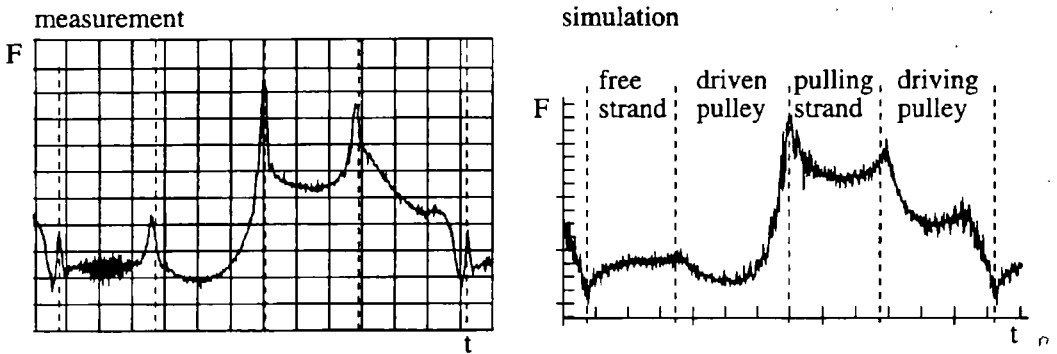


Figure 10. Tensile force in the clasp plate.

force in a clasp plate (left-hand side of Figure 10). (Measurements were performed by G. Sauer and K. T. Renius, Lehrstuhl für Landmaschinen, Technische Universität München.) Therefore, it is necessary to determine the distribution of the tensile force on the plates of the chain links. Using the results of the dynamic simulation shown in Figure 9, and modeling the pair of rocker pins as bending beams and the plates as linear springs, we get the graph of the clasp plate in the right-hand side of Figure 10. The comparison of simulation and measurement confirms the mechanical model.

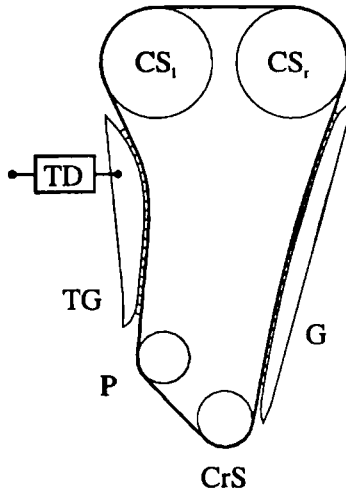


Figure 11. Configuration of a typical roller chain drive.

4.2. Roller Chains in a Car Drive System

In combustion engines, chain drives are used as a driving unit for camshafts and injection pumps. The chain drive is composed of several sprockets (crankshaft, camshafts) and several guides. Figure 11 portrays a typical configuration, which is the basis of the theoretical and experimental research.

The chain consists of 120 links with 360 degrees of freedom. The crankshaft (CrS) is excited by a rotational vibration. The camshafts (CS) are loaded by torques resulting from the valve drive system. These torques are known from measurement. On the tight side of the chain drive, the guide (G) is inertially fixed; on the other side, the tension guide (TG) possesses 1 rotational degree of freedom.

One cycle of a chain link is presented in Figure 12. The first graph shows the contact forces between the link and the sprockets or guides. Regarding the contact between a link and a sprocket, the typical march of the contact force can be seen clearly. At the beginning and the end of the contact phase, a peak in the contact force exists due to the stress of the chain strands. These forces decrease rapidly when the link moves along the teeth of the sprocket. Because of the low curvature of the guide, these contact forces are on a very low level.

The second graph presents the chain stress of one link. The time history mainly follows the torque excitation of the valve drive unit. The effects of the polygonal excitation of the sprocket result in additional forces with small amplitudes. On the tight side of the chain drive, the average forces are twice as large as the forces on the slack side. Figure 13 presents a comparison between measurement and simulation. The first two graphs show the frequency spectra of the motion of the tension guide and the force of the tension device measured at the engine. The next two graphs display the simulation results, which show good agreement with the measurements.

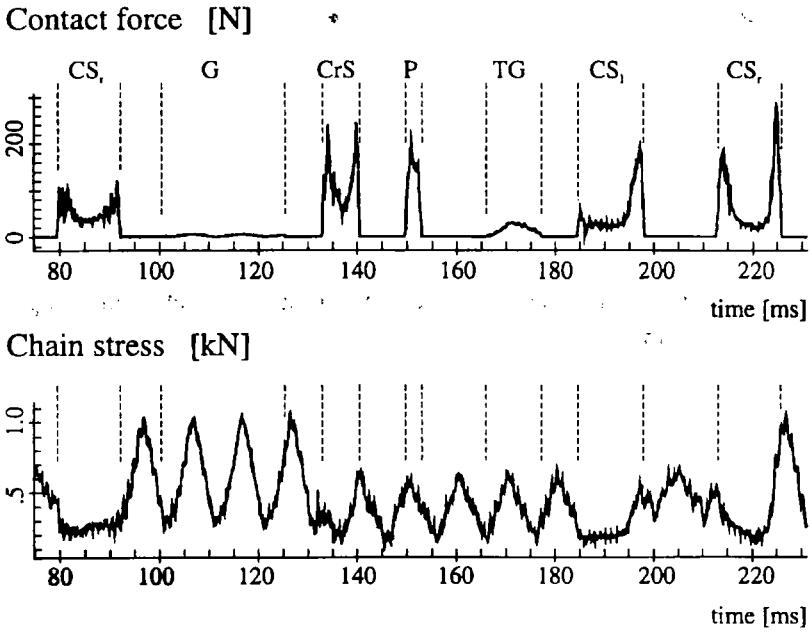


Figure 12. One cycle of a link.

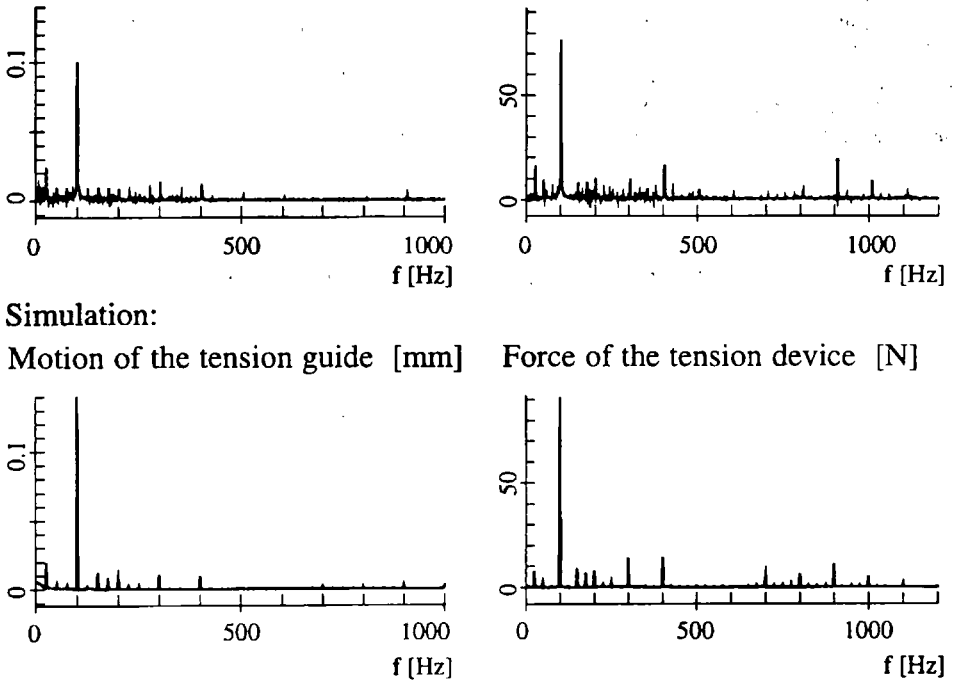


Figure 13. Theory and measurement for a four-stroke engine.

5. SUMMARY

The dynamics of chains are investigated by applying multibody theory in connection with contact mechanical properties. The problem of multiple and nondecoupled contacts typical of chains affords a special treatment of multibody systems, including aspects of linear and nonlinear complementarity theories. The availability of such tools is an indispensable prerequisite for modeling complex systems like chains with their numerous impulsive and friction-induced contact processes. The related theory is presented and applied to two cases: rocker pin chains in CVT gears and roller chains in cars. Results and comparisons with measurements confirm this method of modeling such systems. Further research should be invested in numerical and computer time problems.

REFERENCES

- Binder, R. C., 1956, *Mechanics of the Roller Chain Drive*, Prentice Hall, Englewood Cliffs, NJ.
- Chen, C. K. and Freudenstein, F., 1988, "Towards a more exact kinematics of roller chain drives," *ASME, J Mechan., Trans., Auto. Des.* **110**, 169-275.
- Fritz, P. and Pfeiffer, F., 1995, "Dynamics of high speed roller chain drives," *Proceedings of the 15th Biennial Conference on Mechanical Vibrations and Noise*, Boston, MA, September 17-21.
- Fritzer, A., 1992, "Nichtlineare Dynamik von Steuertrieben," VDI-Fortschrittsberichte, Reihe 11, Nr.176, VDI-Verlag, Düsseldorf.
- Glocker, C. and Pfeiffer, F., 1993, "Complementarity problems in multibody systems with planar friction," *Arch. Appl. Mech.* **63**, 452-463.
- Glocker, C. and Pfeiffer, F., 1995, "Multiple impacts with friction in rigid multibody systems," *Nonlinear Dynamics* **7**, 471-497.
- Lemke, C. E., 1970, "Recent results on complementarity problems," in *Nonlinear Programming*, J. B. Rosen et al., eds., Academic Press, New York, pp. 349-384.
- Mahaligham, S., 1958, "Polygonal action in chain drives," *J. Franklin Inst.* **256**(1), 23-28.
- Naja, M. R. and Marshek, K. M., 1983, "Analysis of the sprocket load distribution," *Mechan. Machine Theory* **18**(5), 349-356.
- Nakanishi, T. and Shabana, A. A., 1994, "Contact forces in the nonlinear dynamic analysis of tracked vehicles," *Int. J. Numerical Methods Eng.* **37**, 1251-1275.
- Pfeiffer, F., 1984, "Mechanische Systeme mit unstetigen Übergängen," *Ingenieur-Archiv* **54**, 232-240.
- Pfeiffer, F., 1993, "Complementarity problems of stick-slip vibrations, dynamics and vibrations of time-varying systems and structures," *ASME* **56**, 43-50.
- Pfeiffer, F. and Glocker, C., 1996, *Multibody Dynamics With Unilateral Contacts*, John Wiley, New York.
- Prestl, W., 1991, "Zahnhämmern in Rädertrieben von Dieselmotoren," *VDI Fortschrittsberichte Reihe 11, Nr.145*, VDI-Verlag, Düsseldorf.
- Seyfferth, W. and Pfeiffer, F., 1992, "Dynamics of rigid and flexible part mating with a manipulator," in *Proceedings of the IMACS-IFAC Symposium*, Lille, 1991, pp. 419-424.
- Smik, J. and Pfeiffer, F., 1994, "Simulation of a CVT chain drive as a multibody system with variant structure," *CISS-First Conference of International Simulation Societies*, Zürich, August 22-25.
- Yue, G., 1992, "Belt vibration consideration moving contact and parametric excitation," in *Proceedings of the International Power Transmission and Gearing Conference* **1**, 311-318.